Battery Bidding and Efficiency in Electricity Market

Hunt Allcott Luming Chen Julia Park*

January 2026

Click here for the latest version.

Preliminary and incomplete. Please do not cite or circulate.

Abstract

Utility-scale batteries play an active role in electricity markets by arbitraging energy across time, yet their efficiency depends critically on market design. This paper studies a prevalent design in real-time electricity auctions: bid lead time, which requires batteries commit bids in advance. Using comprehensive 15-minute bidding and settlement data for all utility-scale batteries in ERCOT from 2018–2024, we document active dynamic bidding, rapid responses to shocks, and the importance of recent price information for forecasting. We develop a dynamic intra-day bidding model with state-of-charge constraints and show that longer bid lead times substantially reduce operational efficiency and profits. Allowing state-of-charge–dependent bids significantly mitigates these losses. Our results highlight bid lead time as a key determinant of battery performance and market outcomes.

*Allcott: Stanford University and NBER, email: allcott@stanford.edu; Chen: University of Michigan, email: lumingch@umich.edu; Park: Stanford University, email: julpark@stanford.edu. We are grateful for comments and suggestions by participants at the Energy Camp, UM/MSU EEE Day, and ISO-NE Market Design workshop. Comments are welcome.

1 Introduction

Utility-scale batteries have expanded rapidly in capacity in the United States and play a critical role in the energy transition. In wholesale electricity markets, batteries serve dual functions: they store energy to complement intermittent renewable generation and act as energy arbitrageurs that smooth intra-day price fluctuations. Batteries actively participate in real-time energy auctions, charging when prices are low and discharging when prices are high. The efficiency of these bidding strategies depends critically on the information available to forecast future prices and optimally time charging and discharging decisions. Despite growing economic interests in energy storages, limited attention has been paid to how batteries operate in electricity markets, how efficiently they bid as energy arbitrageurs, and how bidding (in)efficiencies affect market equilibrium and the broader energy transition.

This paper investigates a key market design feature of real-time electricity auctions that is particularly relevant to battery bidding: the bid lead time, defined as how far advanced batteries should commit their bids. The bid lead time is a common design in the wholesale electricity market around the world and varies across markets. For example, in California ISO (CAISO), batteries need to submit bids for every 60-minute period, commit 75 minutes before start of period, whereas in MidContinent Independent System Operator (MISO), Southwest Power Pool (SPP), and ISO New England (ISO-NE), batteries need to commit their bids 30 minutes in advance. Bid lead time has also received regulatory attention. The CAISO Market Surveillance Committee, for example, has noted that "CAISO should implement rules that enable battery operators to more efficiently manage their state of charge over the day, such as more frequent offer price or limit changes with shorter time lags, state of charge dependent bids and offers, and/or perhaps other design changes." The bid lead time affects bidding efficiency through two primary mechanisms. First, it limits access to the most recent price information, reducing the accuracy of price forecasts. Second, it constrains the flexibility of adjusting the state of charge, further diminishing the efficiency of battery operations. We evaluate how bid lead time shaping battery bidding efficiency in the context of Electric Reliability Council of Texas (ERCOT), where rapidly expanding storage capacity and detailed high-frequency bidding data provides an ideal setting to study battery bidding behavior and real-time market designs.

We compile a comprehensive data set covering all utility-scale batteries in ERCOT from 2018 to 2024, and we access the real-time bidding and settlement information for every 15 minutes. Using these high-frequency data, we document three key data patterns. First, we find that batteries are actively bidding into the real-time energy market to charge during low-price periods and discharge during high-price periods to maximize profits. Batteries submit high generation bid prices to avoid being dispatched too early and to preserve the high option value of stored energy. As

prices approach their peak, batteries sharply lower generation bid prices to ensure dispatch and capture high market prices. Second, we find that batteries respond to unexpected market shocks by quickly increasing the generation bid prices. This behavior demonstrates that batteries actively exploit the real-time information and flexibly adjust their bidding strategy to accommodate the unexpected changes in market conditions. Third, since accurate prediction of future prices is a key prerequisite for batteries to earn profits, we demonstrate a critical role of recent price information in reducing forecast errors.

Motivated by these empirical facts, we develop a dynamic model of battery bidding in which storage operators submit both generation and load bids every 15 minutes, accounting for the evolution of electricity prices and the state of charge. We focus on batteries' bidding problem within a day, allowing the intra-day dynamic problem to be non-stationary, and assume it to be stationary across days. Batteries track their own state of charge, and forecast the future prices with a parsimonious Markov process. Under bid lead time, batteries are required to forecast both future prices and the distribution of state of charge in advance. We solve the resulting non-stationary intra-day dynamic programming using backward induction in an inner loop, and iterate on value functions across days in an outer loop. One key computational challenge is tracking previously committed bid functions, which shape the future distribution of state of charge. As the bid lead time further extends, the state space grows exponentially with the number of advance intervals. To maintain tractability of the dynamic problem, we construct an alternative state representation based on the probability distribution over a discretized state of charge space.

Using the simulated bid functions, we quantify the inefficiency induced by bid lead time. We find that, relative to last-minute bidding, batteries tend to submit lower generation bid prices throughout the day under longer lead time. This occurs because a larger dispersion in the projected price distribution increases the density of tails, which are the primary drivers of batteries' expected profits. Moreover, the average generation bid prices exhibit less intraday variation across intervals, as the increased uncertainty in price forecasts dampens hour-to-hour differences in price forecast. Consequently, batteries are more likely to be discharged earlier in the day but supply less energy during peak-price periods, leading to a substantial deviation from optimal charging-discharging pattern under last-minute bidding. We document a sharp profit-lead horizon gradient. The baseline simulated profit under zero lead time is \$35.8 per kW of installed capacity. Under 30-minute bid lead time as currently implemented in MISO, SPP, and ISO-NE, the average profit is reduced to \$21.7 per kW, which is only 61% of the baseline profit. Under 75-minute bid lead time as currently implemented in CAISO, the average profit is reduced to \$13.4 per kW, which is only 37% of the baseline profit. This result highlights the importance of bidding horizon in shaping operational profits for batteries.

Next, we explore a commonly discussed regulatory proposal of state-of-charge-dependent bids

such that batteries could submit a contingent bid price dependent on the realized state of charge. Due to computation limitations, we evaluate a parsimonious two-point SoC-dependent bids. We find that SoC-dependent bids brings substantial improvement to batteries' operation profits, since SoC-dependent bids mitigates quantity uncertainty and allow contingent plans based on different realizations of state of charge. Under 30-minute bid lead time, SoC-dependent bids improve the average profit by 12%, and close the gap from the baseline profit by 7.2 percentage points (60.5% to 67.7%). Under 75-minute bid lead time, SoC-dependent bids improve the average profit by 42%, and close the gap from the baseline profit by 15.7 percentage points (37.5% to 53.2%).

This paper contributes to the following two strands of literature. First, this is the first economics paper, to out knowledge, empirically evaluate batteries dynamic bidding behavior, which is critical to the market equilibrium. Our paper moves away from common assumptions that batteries are perfect energy arbitrageurs and building in inefficiency from regulatory environment such that their operation might be compromised. Our paper thus complements previous work on the economic values of energy storages, including Butters et al. (2025), Holland et al. (2024), Karaduman (2021), and Lamp and Samano (2022). There are also previous work exploring the market power (Andrés-Cerezo and Fabra, 2023b), complementarity with renewable energy (Andrés-Cerezo and Fabra, 2023a), and congestion benefits (Kirkpatrick, 2020).

Second, this paper investigates the design of wholesale electricity market by extending the analyses to battery bidding. Previous papers have examined strategic bidding (Hortaçsu and Puller, 2008), sequential market (Ito and Reguant, 2016), real-time pricing (Allcott, 2012), bidding sophistication (Hortaçsu et al., 2019), forward commodity markets (Jha and Wolak, 2023). This paper incorporates the bidding behavior of energy storages, highlight the unique dynamic feature, and explore the importance of a common market design feature as well as its solutions.

2 Background

Energy storage has become increasingly more important in the wholesale electricity market. As shown in Figure 1, total generation from wind and solar power in the United States has risen from a negligible level in early 2000s to more than 1,000 TWh in 2020. Utility-scale battery capacity expanded gradually after 2010 and experienced rapid growth after 2020. Texas now hosts the second largest battery capacity in the US, following California. Unlike California, where batteries are often co-located with solar farms and are predominantly four-hour systems, batteries in Texas are mostly stand-alone facilities and are primarily one-hour or two-hour batteries.

Batteries play dual roles in wholesale electricity markets. First, they store energy and complement intermittent renewable generation. First, they store energy and complement intermittent renewable generation. Because wind and solar output often peak at times that do not coincide with

peak electricity demand, batteries can shift energy across time by charging during periods of high renewable generation and discharging during periods of high demand. Second, batteries act as energy arbitrageurs. By charging when prices are low and discharging when prices are high, batteries smooth intra-day price fluctuations. Batteries in ERCOT participate in both the day-ahead market, primarily to provide ancillary services, and the real-time market for energy arbitrage. We focus on the energy arbitrage in the real-time market in this paper.

Batteries actively participate in the wholesale auctions every five minutes, with settlements occurring every fifteen minutes. In each interval, a battery submits a generation bid to supply energy and a load bid to demand energy. These bids are interval- and unit-specific step functions. We illustrate the shape of bid functions for one of the largest batteries in ERCOT, TURQBESS_BESS1, on one hot summer day in 2023, as shown in Appendix Figure A2 and A3. Generation bid prices indicate the minimum price that batteries are willingness to supply a certain amount of energy. They are capped from above at $5,000 per MWh, and a generation bid price at the cap could effectively avoid dispatch. Load bid prices indicate the maximum price that batteries are willingness to accept to demand a certain amount of energy. They are capped from below at -$250 per MWh, and a load bid price at the floor could effectively avoid charging.

To fully exploit arbitrage opportunities, batteries face a complex dynamic decision of when to charge and when to discharge at high frequency, which requires forecasting future prices. However, increasing penetration of renewable energy exacerbates price volatility, making accurate forecasting more difficult. We measure price volatility using the dispersion between real-time and day-ahead market prices, where the day-ahead price is settled before the real-time market opens and is therefore known to batteries at the time of bidding. We observe a clear increase in this dispersion over time as shown in Appendix Figure A1, indicating growing difficulty in forecasting future prices.

Moreover, the design of the auctions might further impede efficient battery bidding. We focus on one such feature: the bid lead time, defined as how far advanced batteries should commit their bids. The bid lead time is a common design in the wholesale electricity market around the world, and it varies across markets. For example, in CAISO, batteries need to submit bids for every 60-minute period, commit 75 minutes before start of period, whereas in MISO, SPP, and ISO New England, batteries need to commit their bids 30 minutes in advance. Bid lead time has also received regulatory attention. The CAISO Market Surveillance Committee, for example, has noted that "CAISO should implement rules that enable battery operators to more efficiently manage their state of charge over the day, such as more frequent offer price or limit changes with shorter time lags, state of charge dependent bids and offers, and/or perhaps other design changes."

Figure 1: Market Evolution of Renewable Generation and Battery Capacity

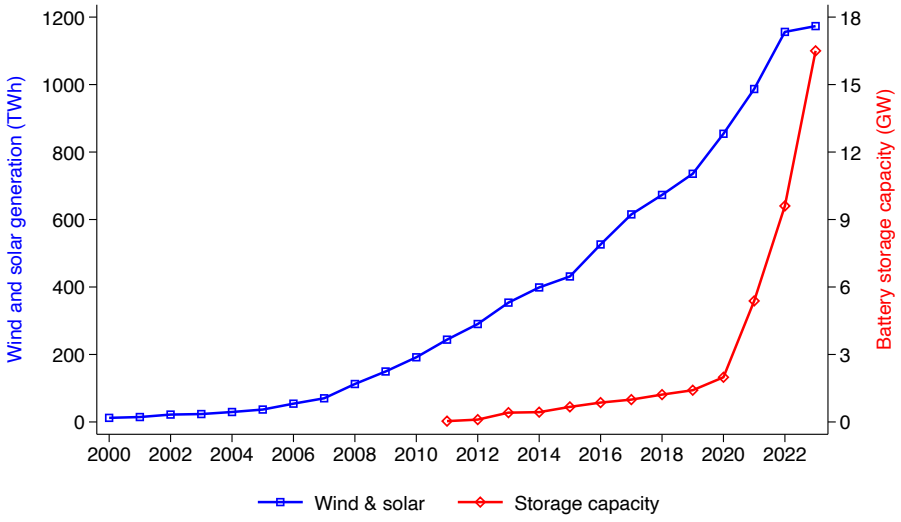

Notes: This figure plots the time trend of wind and solar generation (in blue, y-axis on the left) and the battery capacity (in red, y-axis on the right) in the US from 2000 to 2023.

3 Data and Descriptive Evidence

3.1 Data

We compile a comprehensive data set covering all utility-scale batteries in ERCOT from 2018 to 2024. The data set covers both the day-ahead market including ancillary services and the real-time market. We access the detailed generation bids (submitted to supply electricity), load bids (submitted to demand electricity), bid awards, and real-time market prices at 15-minute frequency. The day-ahead bids for energy and for ancillary services are at hourly frequency, together with hourly awards and prices.

We complement the bidding data with battery information from Energy Information Administration (EIA). We access information such as battery capacity, durations, locations in EIA-860.

3.2 Stylized Facts

Fact 1: Batteries bid dynamically and option value matters

We document dynamic battery bidding patterns as shown in Figure 2. For each 15-minute interval of the day, we compute the average quantity-weighted generation and load bid prices. The ERCOT real-time market price exhibit two daily peaks: a modest morning peak around 7 a.m.,

and a much larger evening peak around 7 p.m., coinciding with periods of high electricity demand. In response to this intraday price variation, batteries dynamically adjust both their generation bid prices and load bid prices. Generation bid prices capture batteries' willingness to sell energy and a high generation bid price will decrease the likelihood of dispatch. Load bid prices capture batteries' willingness to buy energy and a high load bid price will increase the likelihood of being charged.

As shown in Panel (a), we find that batteries tend to submit a high generation bid price several hours before the peak period to avoid being discharged too early, because the option value of stored energy is high. It's more profitable to retain energy for later, higher-price hours, than selling during periods of relatively low market prices. Around the price peak, batteries sharply reduce their generation bid price to ensure that they will be dispatched and energy is sold at a high price. Compared to the generation bid price, we find that the load bid price rises until two to three hours before prices spike and then returns to a lower level, which guarantee that batteries will be fully charged at a low price.

Consistent with the bidding strategy, the average net supply, defined as the difference between the total discharged energy and charged energy, closely track the price pattern, as shown in Panel (b). Batteries are net energy suppliers for morning and evening peak hours, and net energy consumers during the rest of the day.

Overall, these patterns reveal a clear dynamic bidding behavior of batteries. They are actively bidding into the real-time energy market to charge during low-price periods and discharge during high-price periods to maximize profits.

Figure 2: Bid Prices and Net Energy Supply of Batteries

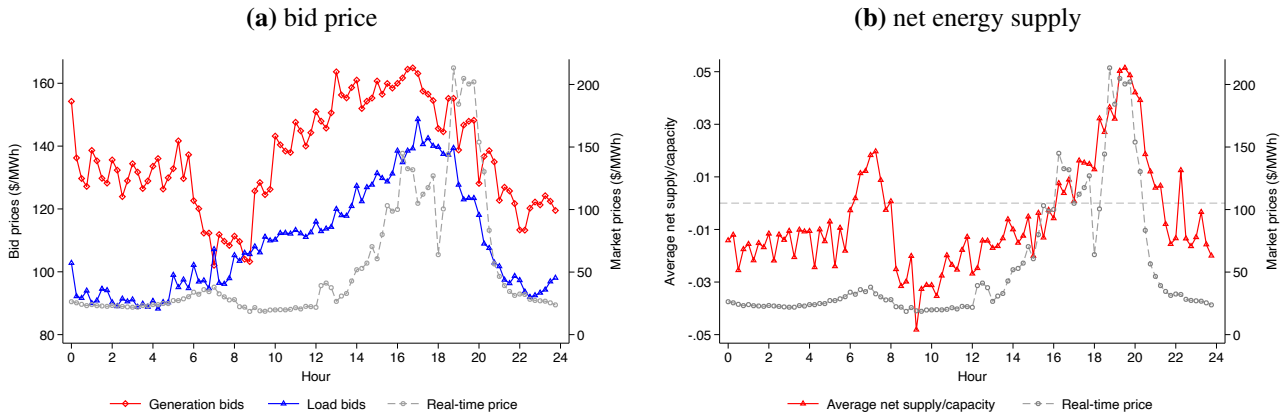

Notes: This figure plots the quantity-weighted average bid prices (Panel (a)) and the net energy supply as a share of capacity (Panel (b)) in 2023. We truncate both generation and load bid prices at an upper bound of $1,000/MWh and winsorize them at a lower bound of -$100/MWh. Real-time market prices are plotted in grey with y-axis on the right for both panels.

Fact 2: Batteries respond to unexpected market shocks

We examine how batteries respond to unexpected market shocks. We identify such shocks at the settlement-point and 15-minute-interval level, combining two sources of unexpected events. The first type consists of unplanned generator or transmission outages that last for more than two hours. The second type captures sudden changes in market conditions. Specifically, we classify an interval as when a shock occurred if the real-time market price exceeds the day-ahead market price by at least 100 dollars/MWh, while real-time–day-ahead price spread remains within $[-50, 50]$ dollars/MWh for the three hours preceding the interval. These criterion isolates intervals during which the real-time prices abruptly deviate from day-ahead prices despite relatively stable spread in the immediate pre-shock period.

We estimate the following event-study specification to evaluate how batteries respond to unexpected market shocks.

$$y_{it} = \sum_{k=-12, k\neq -1}^{12} \beta_k \mathbb{1}(T_{it} = k) + \alpha DAMPrice_{it} + X_{it} + \epsilon_{it}. \tag{1}$$

We index battery by i and 15-minute intervals by t. The dependent variable y_{it} denotes key outcome variables, including market prices and bid prices. T_{it} represents event time relative to the start of a market shock, with $k = -1$ omitted as the reference period. Our key coefficients of interest is β_k, which measures how unexpected market shocks affect the dependent variable k intervals relative to the onset of the shock. We control for day-ahead market prices $DAMPrice_{it}$, and include a rich set of fixed effects X_{it}, consisting of battery fixed effects interacted with month and hour dummies. These fixed effects absorb battery characteristics, seasonality in electricity demand, intra-day volatility, as well as variations in generation resource mixes around each battery. The key identification assumption is that, conditional on the rich controls of day-ahead market prices and unobserved shocks at the battery, month, and hour levels, the timing of market shocks is exogenous to individual batteries.

Figure 3: The Impacts of Unexpected Market Shocks

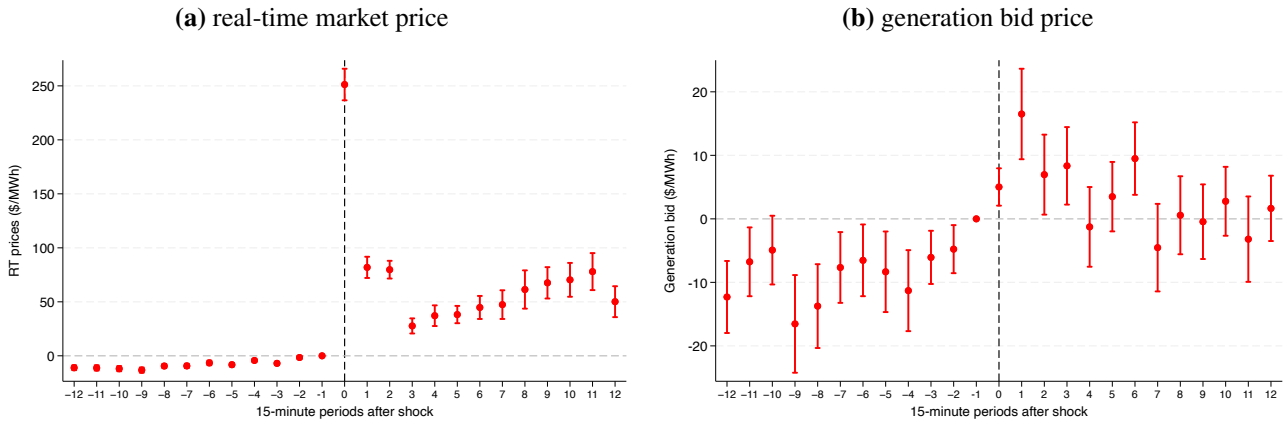

Notes: This figure plots the estimation results of equation (1). Panel (a) plots the impacts of unexpected market shocks on real-time prices, while panel (b) plots the coefficients on generation bid prices. 95% confidence intervals are constructed from clustered standard errors at the battery level.

The event-study estimation results are presented in Figure 3. We confirm that our identified unexpected market shocks drive price spikes in Panel (a), as we observe an abrupt rise in real-time market price at the onset of the shock, and the increase in the price level lasts for more than three hours. On the contrary, we observe a stable level of the real-time market price before the event. More importantly, we find that batteries respond to such shocks by increasing the generation bid levels. This behavior demonstrates that batteries actively exploit the real-time information and flexibly adjust their bidding strategy to accommodate the unexpected changes in market conditions.

Fact 3: Recent prices are most informative for price projections

We investigate the role of recent price information in forming expectations about future prices. Using real-time market prices at a 5-minute frequency, we estimate the following empirical specification to evaluate how much variation in current prices can be explained by past price information.

$$logp_{d,h} = \sum_{h=1}^{288} \gamma_h logp_{d,h-\tau} + \phi DAMPrice_{d,h} + X_{d,h} + \epsilon^{\tau}_{d,h}. \tag{2}$$

We use d and $h$to denote a date and a intra-day five-minute interval, respectively. The dependent variable is the log real-time marker price at day d and interval h, and the key independent variable is the log real-time marker price τ intervals earlier. We allow the coefficients on lagged prices to

vary flexibly across intra-day intervals. Moreover, we control for hourly day-ahead market prices $DAMPrice_{d,h}$, and include month fixed effects to absorb seasonal variation in prices.

The main results are summarized in Figure 4. Panel (a) plots the distribution of prediction errors $\hat{\epsilon}^{\tau}_{d,h}$ when τ= 3 (a 15-minute-ahead prediction) and when $\tau = 15$ (a 75-minute-ahead prediction). Extending the forecasting horizon from 15 minutes to 75 minutes substantially increases the dispersion of prediction errors, with the standard deviation rising by 39.4%. Panel (b) plots the average absolute prediction errors as a function of forecasting horizon, and we find a sharp rise especially within the first two hours. This exercise highlights the importance of recent price information on accurately predicting future real-time prices.

Figure 4: Projection Errors of Prices

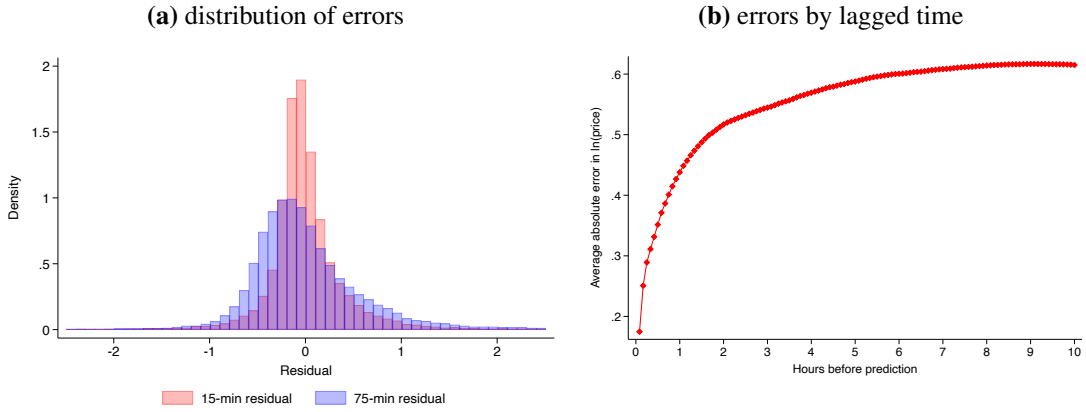

Notes: This figure plots the estimation results of equation (2). Panel (a) plots the distribution of forecast errors when τ= 3 (a 15-minute-ahead prediction) and when $\tau = 15$ (a 75-minute-ahead prediction), while panel (b) plots plots the average absolute prediction errors as a function of forecasting horizon.

Taking stock, these empirical patterns document batteries' dynamic bidding incentives and illustrate how batteries adjust bid prices to exploit intra-day price volatility to maximize profits. Moreover, we also show that batteries respond rapidly to unexpected market shocks in the real-time market. Accurate prediction of future prices is a key prerequisite for earning profits, and we document the critical role of recent price information in reducing forecast errors. These findings further motivate our structural model, in which we characterize batteries' dynamic bidding behavior in the real-time market, and analyze how batteries optimally adjust their bids in the presence of bid lead times that restrict the effective prediction horizon.

4 Structural Model

4.1 Dynamic Bidding of Batteries

We index batteries by i, each with capacity k_i, defined as the maximum amount of power the battery i can discharge. Time is discretized at a 15-minute frequency. We denote each day as d, and each intra-day interval as $h \in \{1, 2, 3, ..., 96\}$. We use t to represent a specific 15-minute interval h on a day d. At the beginning of each interval t, battery i has a remaining state of charge s_{it}, and submits a load bid $\mathcal{B}^l_{it}$ (to get charged) and a generation bid $\mathcal{B}^g_{it}$ (to get discharged). Bids are interval- and unit-specific step functions. For tractability, we assume that batteries submit a single generation bid price b^g_{it} and load bid price b^l_{it} with exogenous and constant bid quantities q^g_i and q^l_i for each interval. b^g_{it} represents the generation bids such that the battery is willing to supply power q^g_i when the real-time market price is above b^g_{it}. Similarly, b^l_{it} represents the load bids such that the battery is willing to buy power q^l_i when the real-time market price is below b^l_{it}.

We denote the real-time market price in interval h as p_h, which follows a Markov process $F_h(p_h|p_{h-1})$. Specifically, we assume that

$$p_h = \theta_h p_{h-1} + \epsilon_h, \tag{3}$$

where ϵ_h follows a skewed normal distribution with mean μ_h, standard deviation σ_h, and skew parameter α_h. For the rest of illustration of the model, we focus on batteries' bidding problem within a specific day, and the dynamic problem is assumed to be stationary across days. Therefore, we substitute all time stamps t with intra-day interval h. Since it's a single-agent dynamic problem, the subscript i is also suppressed. For simplicity, we abbreviate $F_h(p_h|p_{h-1})$ as $F_h(p_h)$.

We begin by formulating the bidding problem for one-hour batteries of 10 MW capacity k_i and discretize the state-of-charge (SoC) space s_h into five values: $\{0, 0.25, 0.5, 0.75, 1\}$. The grid discretization is consistent with the 15-minute bidding frequency, implying that a one-hour battery can charge or discharge one-quarter of its energy capacity in each interval. The round-trip efficiency parameter is $\delta < 1$, which is defined as the ratio of discharged energy to charged energy and measures the efficiency loss in the cycle. Since batteries are subject to the physical constraints such that they can only discharge until SoC = 0 and can only charge up to full, the bidding quantities can be defined as follows.

$$q^g_h = 0.25 \times k_i \times \mathbb{1}(s_h > 0), \quad q^l_h = \frac{0.25 \times k_i}{\delta} \times \mathbb{1}(s_h < 1).$$

The awarded quantity is denoted by a_h. a_h takes a positive value if charging and negative if discharging such that $a_h = -q^g_h \mathbb{1}(p_h \geqslant b^g_h) + q^l_h \mathbb{1}(b^l_h \geqslant p_h)$. The probability distribution of a_h is

given by the follows.

$$P_h(a_h) = \begin{cases} 1 - F_h(b_h^g), & a_h = -q_h^g \\ F_h(b_h^l), & a_h = q_h^l \\ F_h(b_h^g) - F(b_h^l), & a_h = 0 \end{cases}$$

We parameterize the cycling cost $c(\frac{a_h}{k}) = \frac{\zeta|a_h|}{k}$, which is a one-segment special case of the piece-wise linear functional form in Xu et al. (2017), and ζ denotes the unit cycling cost. Therefore, the expected profit function is defined as follows, which is the difference between revenues from discharged energy and cost from charged energy, minus the cycling cost.

$$\begin{aligned} \mathbb{E}_h[\pi(\mathcal{B}_h)] &= \mathbb{E}_h[-a_h \times p_h - \frac{\zeta|a_h|}{k}] \\ &= \mathbb{E}_h\{[q_h^g \mathbb{1}(p_h \geqslant b_h^g) - q_h^l \mathbb{1}(b_h^l \geqslant p_h)]p_h - \frac{\zeta \times [q_h^g \mathbb{1}(p_h \geqslant b_h^g) + q_h^l \mathbb{1}(b_h^l \geqslant p_h)]}{k}]\} \\ &= \underbrace{\int_{p_h \geqslant b_h^g} q_h^g p_h dF_h(p_h)}_{\text{revenues from discharging}} - \underbrace{\int_{p_h \leqslant b_h^l} q_h^l p_h dF_h(p_h)}_{\text{costs from charging}} - \underbrace{\frac{\zeta \times [q_h^g(1 - F_h(b_h^g)) + q_h^l F_h(b_h^l)]}{k}}_{\text{cycling cost}}. \end{aligned} \quad (4)$$

The expected transition dynamics of s_h is defined as follows with round-trip efficiency parameter as $\delta < 1$, $s_{h+1} = s_h - q_h^g \mathbb{1}(p_h \geqslant b_h^g) + \delta q_h^l \mathbb{1}(b_h^l \geqslant p_h)$. The probability distribution of s_{h+1} is given by the follows.

$$P_h(s_{h+1}) = \begin{cases} 1 - F_h(b_h^g), & s_{h+1} = s_h - q_h^g \\ F_h(b_h^l), & s_{h+1} = s_h + \delta q_h^l \\ F_h(b_h^g) - F_h(b_h^l), & s_{h+1} = s_h \end{cases}$$

A battery decides when to charge or discharge by submitting a generation bid price and a load bid price for every interval h. By submitting a lower generation bid price in the current period, batteries are more likely to be dispatched and earn a profit from supplying energy. However, discharging reduces the remaining state of charge, making the battery less able to continue supplying energy in subsequent periods without first recharging. The value function can be formulated as follows with discount factor β. If the price is expected to be high in the current period, batteries tend to submit a low generation bid price b_h^g to guarantee being discharged. If the price is expected to be high in the future periods, batteries tend to submit a high generation bid price b_h^g to avoid being discharged early and might submit a high load bid price b_h^l to ensure recharging. This trade-off is more obvious from the expression of the continuation value in equation (6), as a lower generation

bid price b_h^g increases the profit from the current period, but reduces the continuation value by moving the value function to low SoC state.

$$V_h(s_h, p_{h-1}) = \max_{\mathcal{B}_h}\{ \underbrace{\mathbb{E}_h[\pi(\mathcal{B}_h)]}_{\text{profit from the current period}} + \underbrace{\beta \mathbb{E}_h[V_{h+1}(s_{h+1}, p_h)|s_h, p_{h-1}]}_{\text{continuation value from the future}}\} \tag{5}$$

$$\begin{aligned}\mathbb{E}_h[V_{h+1}(s_{h+1}, p_h)|s_h, p_{h-1}] = \int_{p_h} \{&[1 - F_h(b_h^g)]V_{h+1}(s_h - q_h^g, p_h) + [F_h(b_h^g) - F_h(b_h^l)]V_{h+1}(s_h, p_h) \\ &+ F_h(b_h^l)V_{h+1}(s_h + \delta q_h^l, p_h)\} dF_h(p_h|p_{h-1}).\end{aligned} \tag{6}$$

Therefore, the optimal generation bid price b_h^g can be expressed as follows.

$$b_h^g = \frac{c}{k} + \beta \times \frac{\int_{p_h} [V_{h+1}(s_h, p_h) - V_{h+1}(s_h - q_h^g, p_h)] dF_h(p_h|p_{h-1})}{q_h^g}. \tag{7}$$

Equivalently, the optimal load bid price b_h^l can be expressed as follows.

$$b_h^l = -\frac{c}{k} + \beta \times \frac{\int_{p_h} [V_{h+1}(s_h + \delta q_h^l, p_h) - V_{h+1}(s_h, p_h)] dF_h(p_h|p_{h-1})}{q_h^l}. \tag{8}$$

The optimal bid prices have intuitive interpretations. The optimal generation bid price measures the willingness to discharge for batteries and covers the opportunity cost of discharging early. The optimal load bid price measures the willingness to charge for batteries and captures the average discounted value of extra SoC in the next period. Cycling cost will make bids more conservative and be less likely to result in a quantity award.

4.2 Bidding under Lead Time

We introduce lead time to the bidding problem such that bids for period t must be submitted z periods in advance at the beginning of $t - z$. With a lead time z, batteries need to formulate expectation over p_h conditional on its current price information available at time $h-z$, p_{h-z-1}. We denote the conditional distribution of p_h given p_{h-z-1} as $G_h^z(p_h|p_{h-z-1})$, abbreviated as $G_h^z(p_h)$. The distribution of $G_h^z(p_h)$ evolves recursively according to the underlying one-period price transition kernels $F_{h-k}(\cdot|\cdot)$.

$$G_h^z(p_h \mid p_{h-z-1}) = \int \cdots \int F_h(p_h \mid p_{h-1}) \prod_{j=1}^{z} dF_{h-j}(p_{h-j} \mid p_{h-j-1}), \;\; G_h^0(p_h \mid p_{h-1}) = F_h(p_h \mid p_{h-1})$$

The expected z-period transition dynamics of s_h is a more complicated problem. Every period, there are three potential changes (being discharged, being charged, or staying the same), and thus there would be 3^z possible trajectories during z periods. Those trajectories depend on the current state-of-charge s_{h-z}, price evolution F_h, as well as all interim bid prices that have already been committed $\mathcal{B}_{h-z}$.

$$\mathcal{B}_{h-z} = \{b_{h-z}^g, b_{h-z+1}^g, b_{h-z+2}^g, ..., b_{h-1}^g, b_{h-z}^l, b_{h-z+1}^l, b_{h-z+2}^l, ..., b_{h-1}^l\}.$$

The expected z-period transition dynamics of s_h can be written as follows.

$$P_h^z(s_h \mid s_{h-z}, \mathcal{B}_{h-z}) = \sum_{s_{h-1}} \cdots \sum_{s_{h-z+2}} \sum_{s_{h-z+1}} \prod_{j=-z}^{-1} P_{h+j}(s_{h+j+1} \mid s_{h+j}, b_{h+j}^g, b_{h+j}^l). \tag{9}$$

Consequently, the profit function can be written as follows. Compared to profit functions under last-minute bidding in equation (4), the expected profit under bid lead time requires z-period projection of both prices and SoCs.

$$\begin{aligned} \mathbb{E}_h[\pi(b_h^g, b_h^l, s_{h-z}, p_{h-z-1}, \mathcal{B}_{h-z})] = \sum_{s_h} \{ & \int_{p_h \geqslant b_h^g} q_h^g \times p_h dG_h^z(p_h) - \int_{p_h \leqslant b_h^l} q_h^l \times p_h dG_h^z(p_h) \\ & - \frac{\zeta \times [q_h^g(1 - G_h^z(b_h^g)) + q_h^l G_h^z(b_h^l)]}{k} \} \\ & \times P_h^z(s_h \mid s_{h-z}, p_{h-z-1}, \mathcal{B}_{h-z}). \end{aligned} \tag{10}$$

In period $h - z$, the battery bid for interval h, conditional on its current state-of-charge s_{h-z}, previous-period price p_{h-z-1}, as well as all interim bid prices that are pre-committed $\mathcal{B}_{h-z}$. The value function can be formulated as below

$$\begin{aligned} V_{h-z}(s_{h-z}, p_{h-z-1}, \mathcal{B}_{h-z}) = \max_{b_h^g, b_h^l} \{ & \mathbb{E}_h[\pi(b_h^g, b_h^l, s_{h-z}, p_{h-z-1}, \mathcal{B}_{h-z})] \\ & + \beta \mathbb{E}_h[V_{h-z+1}(s_{h-z+1}, p_{h-z}, \mathcal{B}_{h-z+1}) | b_h^g, b_h^l, s_{h-z}, p_{h-z-1}, \mathcal{B}_{h-z}] \} \end{aligned}$$

However, $\mathcal{B}_{h-z}$ is relatively high-dimensional and challenging to track in dynamic program-

ming. For example, if we consider a bid lead time of 75 minutes, then $\mathcal{B}_{h-z}$ adds 10 more state variables, which imposes a heavy burden on computation.[1] To keep tractability of the dynamic problem, we construct an alternative set of state variables $\Phi(s_{h-z}, p_{h-z-1}, \mathcal{B}_{h-z})$ to reduce the computation burden. The choice of $\Phi(s_{h-z}, p_{h-z-1}, B_{h-z})$ is motivated by the profit function (10). Instead of tracking s_{h-z} and $\mathcal{B}_{h-z}$ individually, we track the probability distribution of s_h. Since we discretize the space of state of charge s_h into five values,$\{0, 0.25, 0.5, 0.75, 1\}$, we track the following five state variables.[2]

$$\tau_h =(\tau_h^1 = P(s_h = 0), \tau_h^2 = P(s_h = 0.25), \tau_h^3 = P(s_h = 0.5), \tau_h^4 = P(s_h = 0.75), \tau_h^5 = P(s_h = 1)).$$

Therefore, $\Phi(s_{h-z}, p_{h-z-1}, \mathcal{B}_{h-z}) = \{\tau_h, p_h\}$. The transition of τ_h follows the evolution rules below.

$$\tau_{h+1} = (\tau_{h+1}^1, \tau_{h+1}^2, \tau_{h+1}^3, \tau_{h+1}^4, \tau_{h+1}^5) = \begin{cases} (\tau_h^1 + \tau_h^2, \tau_h^3, \tau_h^4, \tau_h^5, 0), & 1 - G_h^z(b_h^g) \\ (0, \tau_h^1, \tau_h^2, \tau_h^3, \tau_h^4 + \tau_h^5), & G_h^z(b_h^l) \\ (\tau_h^1, \tau_h^2, \tau_h^3, \tau_h^4, \tau_h^5), & G_h^z(b_h^g) - G_h^z(b_h^l) \end{cases}$$

The profit function and value function can be simplified as follows.

$$\begin{aligned} \mathbb{E}_h[\pi(b_h^g, b_h^l, s_{h-z}, p_{h-z-1}, \mathcal{B}_{h-z})] = &\sum_{s_h}[q_h^g(s_h) \times \tau_h^{s_h}] \int_{p_h \geqslant b_h^g} p_h dG_h^z(p_h) - \sum_{s_h}[q_h^l(s_h) \times \tau_h^{s_h}] \int_{p_h \leqslant b_h^l} p_h dG_h^z(p_h) \\ &- \sum_{s_h} \frac{\zeta \times [q_h^g(s_h) \times \tau_h^{s_h} \times (1 - G_h^z(b_h^g)) + q_h^l(s_h) \times \tau_h^{s_h} \times G_h^z(b_h^l)]}{k}. \end{aligned}$$

$$V_{h-z}(\tau_h, p_{h-z-1}) = \max_{b_h^g, b_h^l} \mathbb{E}_h[\pi_h(b_h^g, b_h^l, \tau_h, p_{h-z-1})] + \beta \mathbb{E}_h[V_{h-z+1}(\tau_{h+1}, p_{h-z})|b_h^g, b_h^l, \tau_h, p_{h-z-1}].$$

The optimal bid prices are as below.

$$b_h^g = \frac{c}{k} + \beta \times \frac{\int_{p_h} [V_{h-z+1}(\tau_h^1, \tau_h^2, \tau_h^3, \tau_h^4, \tau_h^5, p_{h-z}) - V_{h-z+1}(\tau_h^1 + \tau_h^2, \tau_h^3, \tau_h^4, \tau_h^5, 0, p_{h-z})] dG_h^z(p_h|p_{h-z-1})}{\sum_{s_h}[q_h^g(s_h) \times \tau_h^{s_h}]}. \tag{11}$$

[1] If we choose 5 grid points for each state variable, then the total state space will consist of 244 million (5^{12}) combined grid points.

[2] We instead could track a continuous state variable $\bar{s}_h = \mathbb{E}_{h-z}(s_h)$. However, this is not ideal since the profit function is a non-linear function of s_{h-z} and $\mathcal{B}_{h-z}$, and tracking only the mean statistics misses the curvature of the profit function. A downside is the increased computation burdens for short bid lock windows (shorter than 15 minutes), as we would track a relatively sparse $\Phi(s_{h-z}, p_{h-z-1}, \mathcal{B}_{h-z})$. For example, when there is no bid lock window, τ_h^n can only take values of zero or one since the battery knows the exact s_h.

$$b_h^l = -\frac{c}{k} + \beta \times \frac{\int_{p_h} [V_{h-z+1}(0, \tau_h^1, \tau_h^2, \tau_h^3, \tau_h^4 + \tau_h^5, p_{h-z}) - V_{h-z+1}(\tau_h^1, \tau_h^2, \tau_h^3, \tau_h^4, \tau_h^5, p_{h-z})] dG_h^z(p_h|p_{h-z-1})}{\sum_{s_h}[q_h^l(s_h) \times \tau_h^{s_h}]}. \quad (12)$$

Compared with bid price functions without lead time in equations (7) and (8), bid price functions under lead time z in equations (11) and (12) differ in two key aspects. First, batteries must forecast prices further into the future. Because they do not observe the most recent price realization, but only the price from $z+1$ periods earlier, their price projections are inherently noisier. Second, batteries face uncertainty in SoC, which is a joint result of previously committed bids and past realizations of prices. Uncertainty in SoC further exacerbates inefficiency in the bid functions.

5 Estimation

We estimate the $F_h(p_h|p_{h-1})$ via maximum likelihood estimators using the average prices at the 15-minute frequency from 2021 to 2023. Since we allow period-specific parameters in $F_h(p_h|p_{h-1})$ and relatively flexible parametric assumptions on the error term distributions, we are able to fit the mean and standard deviation of prices well, as shown in Appendix Figure A7. We calibrate the round-trip efficiency parameter δ as 0.85, since our granular calibration of δ by battery and month is distributed between 0.65 and 0.95. Moreover, we calibrate the unit degradation cost $\zeta = 500$ dollars per unit of cycling depth, which yields reasonable charging patterns. We plan on estimating degradation cost instead of calibrating it, by matching the model-predicted the average bidding prices across intervals with the data.

To solve batteries' optimal bid prices under various lead time, our estimation takes two steps. First, we construct $G_h^z\left(p_h \mid p_{h-z-1}\right)$ according to the underlying one-period price transition kernels $F_{h-k}(\cdot|\cdot)$. To visualize the price forecast under bid lead time, we simulate future price distributions conditional on mean realized prices each period. As shown in Appendix Figure A8, the mean future prices under various lead time follow closely with the mean future prices without lead time (Panel (a)), while the dispersion of projected prices is much larger as the lead time becomes longer (Panel (b)). Therefore, bid lead time substantially increases the likelihood of tails in the projection of future prices.

Second, we solve the dynamic programming of batteries. We discretize the price space into 32 grid points, and discretize the 5-point probability τ_h into 126 grid points. Since we assume a non-stationary dynamic problem within a day and a stationary dynamic problem across days, we use backward induction in the inner loop, while iterate on value functions for the end period (96^{th} interval of a day) in the outer loop.

6 Counterfactual Simulations

6.1 Bidding under Lead Time

We first investigate how lead time affects batteries' bidding strategies, net energy supply, and profits. We solve the generation and load bid prices under various bid lead time, and then simulate operations of 100 identical one-hour batteries of 10 MW capacity for 300 days by 1,000 times. The results are shown in Figure 5. Relative to last-minute bidding, batteries tend to submit lower generation bid prices throughout the day under longer lead time. This occurs because a larger dispersion in the projected price distribution increases the density of tails, which are the primary drivers of batteries' expected profits. Moreover, the average generation bid prices exhibit less intra-day variation across intervals, as the increased uncertainty in price forecasts dampens hour-to-hour differences in price forecast. Consequently, batteries are more likely to be discharged earlier in the day but supply less energy during peak-price periods, leading to a substantial deviation from optimal charging-discharging pattern under last-minute bidding.

Figure 5: Bids, Energy Supply, Profits under Bid Lead Time

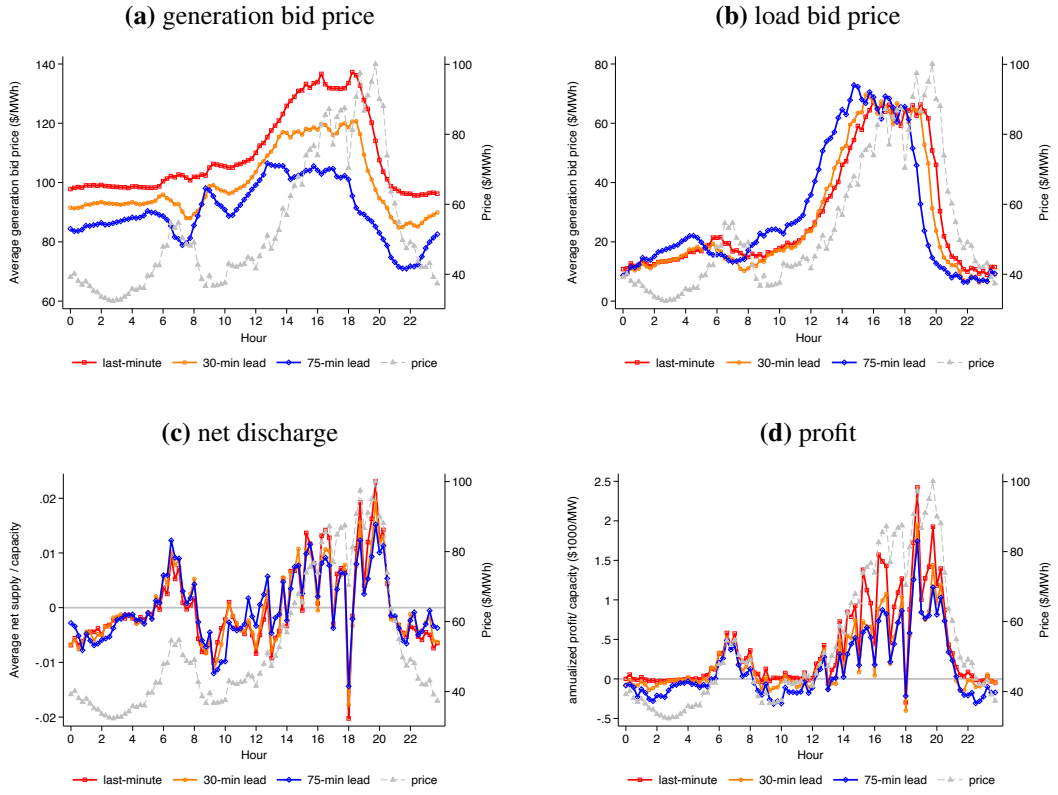

Notes: This figure plots the simulated generation bid prices, load bid prices, net energy supply, and profit at the 15-minute frequency for three scenarios: (1) last-minute bidding (red squares), (2) 30-minute bid lead time (orange circles), and (3) 75-minute bid lead time (blue diamonds). We further plot the real-time market prices in gray.

Moreover, we document a sharp profit-lead horizon gradient as shown in Figure 6. The baseline simulated profit under zero lead time is \$35.8 per kW of installed capacity, which is close to the \$55 per kW of installed capacity as calculated by Modo Energy. Under 30-minute bid lead time as currently implemented in MISO, SPP, and ISO-NE, the average profit is reduced to \$21.7 per kW, which is only 61% of the baseline profit. Under 75-minute bid lead time as currently implemented in CAISO, the average profit is reduced to \$13.4 per kW, which is only 37% of the baseline profit. These results highlights the importance of bidding horizon in shaping operational profits for batteries.

Figure 6: Profits under Bid Lead Time and SoC-dependent Bids

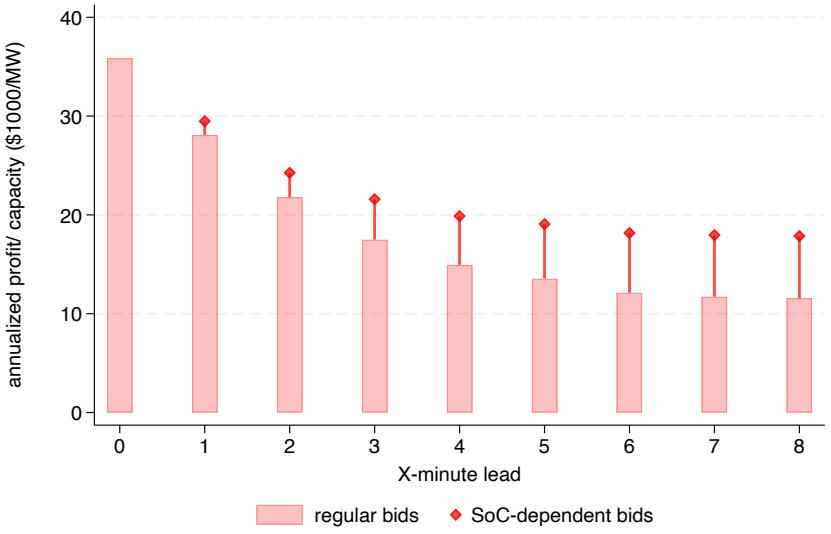

Notes: This figure plots the simulated profits under various bid lead time conditional on mean realized prices each period.

6.2 Bid Lead Time with SoC-dependent Bids

We introduce SoC-dependent bids. Instead of submitting b_h^g and b_h^l, batteries can submit bids as a function of s_t. Since s_t is discretized into five different values (0, 0.25, 0.5, 0.75, 1), b_h^g and b_h^l can each take five different values, denoted by $b_h^g(s_h)$ and $b_h^l(s_h)$. The new profit function is as follows. Compared with 10, the main difference is that now the bid price is SoC dependent.

$$
\begin{aligned}
&\mathbb{E}_h[\pi(b_h^g(s_h), b_h^l(s_h), s_{h-z}, p_{h-z-1}, \mathcal{B}_{h-z})] \\
=&\sum_{s_h}[q_h^g(s_h) \times \tau_h^{s_h}] \times \int\limits_{p_h \geqslant b_h^g(s_h)} p_h dG_h^z(p_h) - \sum_{s_h}[q_h^l(s_h) \times \tau_h^{s_h}] \times \int\limits_{p_h \leqslant b_h^l(s_h)} p_h dG_h^z(p_h) \\
&- \sum_{s_h} \frac{\zeta \times [q_h^g(s_h) \times \tau_h^{s_h} \times (1 - G_h^z(b_h^g(s_h))) + q_h^l(s_h) \times \tau_h^{s_h} \times G_h^z(b_h^l(s_h))]}{k}.
\end{aligned}
$$

However, allowing full flexibility of $b_h^g(s_h)$ and $b_h^l(s_h)$ makes the transition process of τ_h very challenging to specify and code. Therefore, we impose more structures on the state-of-charge dependent bids as follows.

$$
b_h^g = \begin{cases} b_h^{g1}, & s_h \geqslant 0.25 \\ b_h^{g2}, & s_h \geqslant 0.5 \end{cases} \qquad b_h^l = \begin{cases} b_h^{l1}, & s_h \leqslant 0.75 \\ b_h^{l2}, & s_h \leqslant 0.5 \end{cases}
$$

Therefore, we categorize possible state-of-charge into two types: low SoC when SoC is below or equal to 0.25, and high SoC when SoC is above or equal to 0.5. Moreover, we impose another assumption such that

$$
b_h^{g1} \geqslant b_h^{g2} \geqslant b_h^{l2} \geqslant b_h^{l1}
$$

This monotonicity assumption helps us simply the expression of SoC transition dynamics. Moreover, this is intuitive since when SoC is low, batteries are more conservative in bidding to discharge, and when SoC is high, batteries are more conservative in bidding to charge. Under this assumption, we can write the transition dynamics of as follows.

$$
\begin{aligned}
\tau_{h+1} &= (\tau_{h+1}^1, \tau_{h+1}^2, \tau_{h+1}^3, \tau_{h+1}^4, \tau_{h+1}^5) \\
&= \begin{cases} (\tau_h^1 + \tau_h^2, \tau_h^3, \tau_h^4, \tau_h^5, 0), & 1 - G_h^z(b_h^{g1}) \\ (\tau_h^1, \tau_h^2 + \tau_h^3, \tau_h^4, \tau_h^5, 0), & G_h^z(b_h^{g1}) - G_h^z(b_h^{g2}) \\ (\tau_h^1, \tau_h^2, \tau_h^3, \tau_h^4, \tau_h^5), & G(b_h^{g2}) - G_h^z(b_h^{l2}) \\ (0, \tau_h^1, \tau_h^2, \tau_h^3 + \tau_h^4, \tau_h^5), & G(b_h^{l2}) - G_h^z(b_h^{l1}) \\ (0, \tau_h^1, \tau_h^2, \tau_h^3, \tau_h^4 + \tau_h^5), & G_h^z(b_h^{l1}) \end{cases}
\end{aligned}
$$

The value function can be written down as follows.

$$V_{h-z}(\tau_h, p_{h-z-1}) = \max_{b_h^g, b_h^l} \mathbb{E}_h[\pi_h(b_h^g(s_h), b_h^l(s_h), \tau_h, p_{h-z-1})] + \beta \mathbb{E}_h[V_{h-z+1}(\tau_{h+1}, p_{h-z}) | b_h^g(s_h), b_h^l(s_h), \tau_h, p_{h-z-1}]$$

We can derive the first-order conditions as follows.

$$b_h^{g1} = \frac{c}{k} + \frac{\int_{p_h} [V_{h-z+1}(\tau_h^1, \tau_h^2+\tau_h^3, \tau_h^4, \tau_h^5, 0, p_{h-z}) - V_{h-z+1}(\tau_h^1+\tau_h^2, \tau_h^3, \tau_h^4, \tau_h^5, 0, p_{h-z})] dG_h^z(p_h|p_{h-z-1})}{q_h^g(0.25) \times \tau_h^2}.$$

$$b_h^{g2} = \frac{c}{k} + \frac{\int_{p_h} [V_{h-z+1}(\tau_h^1, \tau_h^2, \tau_h^3, \tau_h^4, \tau_h^5, p_{h-z}) - V_{h-z+1}(\tau_h^1, \tau_h^2+\tau_h^3, \tau_h^4, \tau_h^5, 0, p_{h-z})] dG_h^z(p_h|p_{h-z-1})}{q_h^g(0.5) \times (\tau_h^3+\tau_h^4+\tau_h^5)}.$$

$$b_h^{l2} = -\frac{c}{k} + \frac{\int_{p_h} [V_{h-z+1}(0, \tau_h^1, \tau_h^2, \tau_h^3+\tau_h^4, \tau_h^5, p_{h-z}) - V_{h-z+1}(\tau_h^1, \tau_h^2, \tau_h^3, \tau_h^4, \tau_h^5, p_{h-z})] dG_h^z(p_h|p_{h-z-1})}{q_h^l(0) \times (\tau_h^1+\tau_h^2+\tau_h^3)}.$$

$$b_h^{l1} = -\frac{c}{k} + \frac{\int_{p_h} [V_{h-z+1}(0, \tau_h^1, \tau_h^2, \tau_h^3, \tau_h^4+\tau_h^5, p_{h-z}) - V_{h-z+1}(0, \tau_h^1, \tau_h^2, \tau_h^3+\tau_h^4, \tau_h^5, p_{h-z})] dG_h^z(p_h|p_{h-z-1})}{q_h^l(0.75) \times \tau_h^4}.$$

We solve the generation and load bid prices using SoC-dependent bids and under various bid lead time, and then simulate operations of 100 identical one-hour batteries of 10 MW capacity for 300 days by 1,000 times. The average generation bid prices, as shown in Panel (a) of Figure 7, differentiate substantially between the upper level (b_h^{g1}) and lower level (b_h^{g2}) with the regular generation bid prices closer to the lower level. This is intuitive since the potential opportunity cost of discharging will be much higher if the batteries have already been on low state of charge, and allowing state-of-charge dependent bids allow batteries to make contingent plans on realized state of charge and submit more sophisticated bids. Similarly, the average load bid prices are closer to the upper level (b_h^{l2}) with substantial level differences between the upper level (b_h^{l2}) and lower level (b_h^{l1}).

Figure 7: Bids Prices Using SoC-dependent Bids

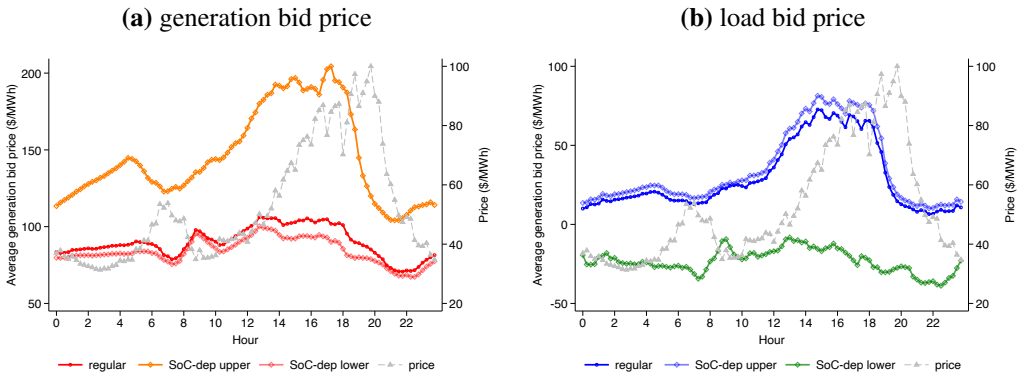

Notes: This figure plots the simulated generation bid prices and load bid prices under 30-minute bid lead time with regular bidding and SoC-dependent bids.

SoC-dependent bids brings substantial improvement to batteries' operation profits, since SoC-dependent bids mitigates quantity uncertainty and allow contingent plans based on different realizations of state of charge. As shown in Figure 6, under 30-minute bid lead time, SoC-dependent bids improve the average profit by 12%, and close the gap from the baseline profit by 7.2 percentage points (60.5% to 67.7%). Under 75-minute bid lead time, SoC-dependent bids improve the average profit by 42%, and close the gap from the baseline profit by 15.7 percentage points (37.5% to 53.2%). The profit-lead horizon gradient is much flatter under SoC-dependent bids. Therefore, allowing contingent bidding plans significantly lowers the uncertainty towards quantities, and improves batteries' operation profits.

7 Conclusion

Utility-scale batteries play a central role in electricity markets by arbitraging energy across time, yet their efficiency depends critically on market design. This paper studies bid lead time in real-time electricity auctions, which requires batteries commit bids in advance. Using comprehensive 15-minute bidding and settlement data for all utility-scale batteries in ERCOT from 2018–2024, we document active dynamic bidding, rapid responses to shocks, and the importance of recent price information for forecasting. We develop a dynamic intra-day bidding model with state-of-charge constraints and show that longer bid lead times substantially reduce operational efficiency and profits. Allowing state-of-charge–dependent bids significantly mitigates these losses. Our results highlight bid lead time as a key determinant of battery performance and market outcomes.

References

Allcott, H. (2012). Real-time pricing and electricity market design. *NBER Working paper*.

Andrés-Cerezo, D. and Fabra, N. (2023a). Storage and renewable energies: Friends or foes. Technical report, Working Paper.

Andrés-Cerezo, D. and Fabra, N. (2023b). Storing power: Market structure matters. *The RAND Journal of Economics*, 54(1):3–53.

Butters, R. A., Dorsey, J., and Gowrisankaran, G. (2025). Soaking up the sun: Battery investment, renewable energy, and market equilibrium. *Econometrica*, 93(3):891–927.

Holland, S. P., Mansur, E. T., and Yates, A. J. (2024). Electrification in the long run. Technical report, Tech. rep. National Bureau of Economic Research.

Hortaçsu, A., Luco, F., Puller, S. L., and Zhu, D. (2019). Does strategic ability affect efficiency? evidence from electricity markets. *American Economic Review*, 109(12):4302–4342.

Hortaçsu, A. and Puller, S. L. (2008). Understanding strategic bidding in multi-unit auctions: a case study of the texas electricity spot market. *The RAND Journal of Economics*, 39(1):86–114.

Ito, K. and Reguant, M. (2016). Sequential markets, market power, and arbitrage. *American Economic Review*, 106(7):1921–1957.

Jha, A. and Wolak, F. A. (2023). Can forward commodity markets improve spot market performance? evidence from wholesale electricity. *American Economic Journal: Economic Policy*, 15(2):292–330.

Karaduman, Ö. (2021). Economics of grid-scale energy storage.

Kirkpatrick, A. J. (2020). Estimating congestion benefits of batteries for unobserved networks: A machine learning approach.

Lamp, S. and Samano, M. (2022). Large-scale battery storage, short-term market outcomes, and arbitrage. *Energy Economics*, 107:105786.

Xu, B., Zhao, J., Zheng, T., Litvinov, E., and Kirschen, D. S. (2017). Factoring the cycle aging cost of batteries participating in electricity markets. *IEEE Transactions on Power Systems*, 33(2):2248–2259.

Online Appendix for
Battery Bidding and Efficiency in Electricity Market

Hunt Allcott Luming Chen Julia Park

A Additional Figures

Figure A1: DART Spread in ERCOT

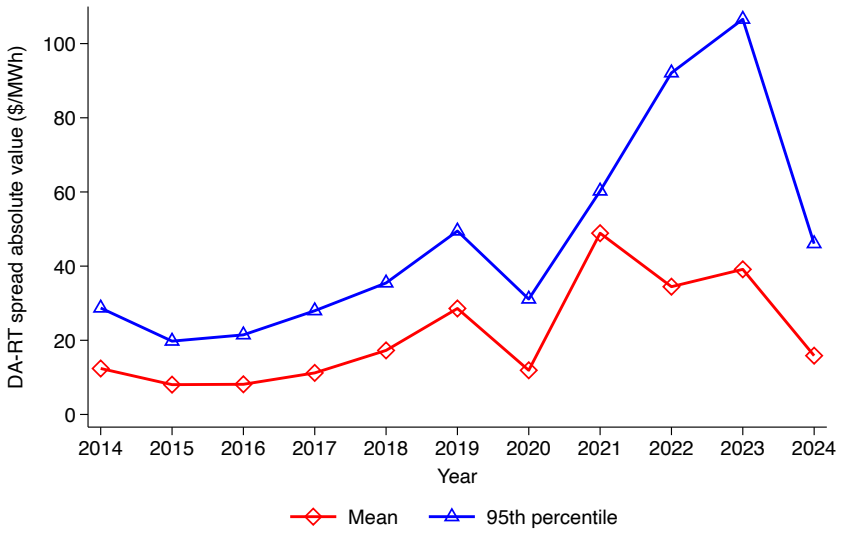

Notes: This figure plots the time series of absolute values of DART spread, which is defined as the difference between the day-ahead market price and real-time market price. We calculate the absolute values of DART spread at 15-minute frequency and calculate the annual averages (red circles) and annual 95^{th} percentiles (blue triangles).

Figure A2: Generation Bids of TURQBESS_BESS1 on September 8, 2023

(a) raw pattern

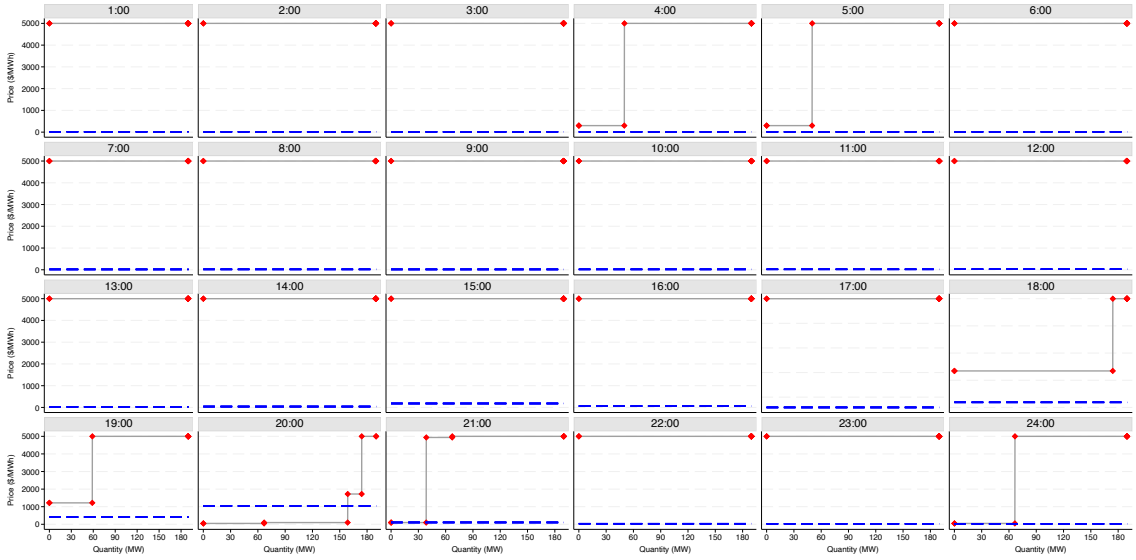

(b) censored bid price

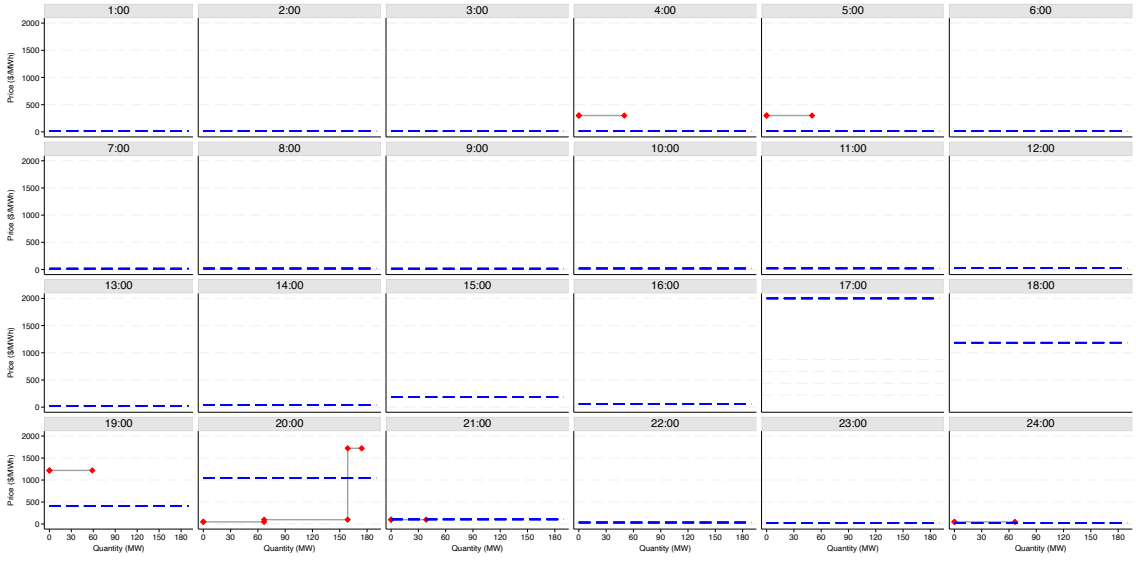

Notes: This figure plots the generation bids submitted by TURQBESS_BESS1, one of the largest utility-scale battery in ERCOT. The bids are submitted on September 8, 2023 when Texas experiences significant heat, with temperatures reaching as high as 107°F in several locations. Panel (a) plots the raw bids and panel (b) plots the truncated bids at -10 dollars/MWh and 2,000 dollars/MWh. We use blue dashed line to denote the average real-time market prices for the corresponding hour in Texas on that day.

Figure A3: Load Bids of TURQBESS_BESS1 on September 8, 2023

(a) raw pattern

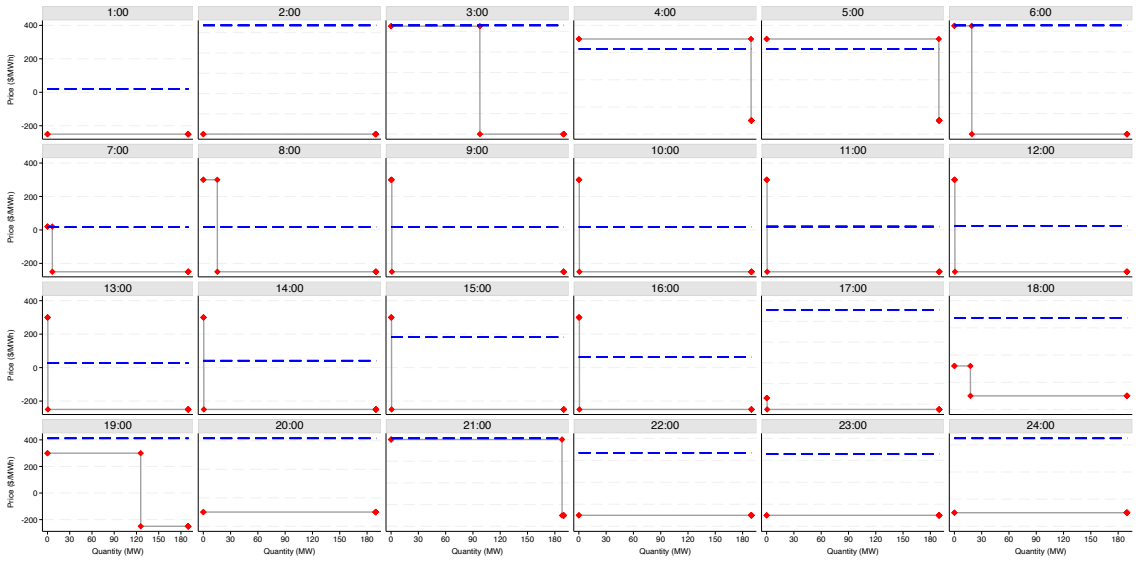

(b) censored bid price

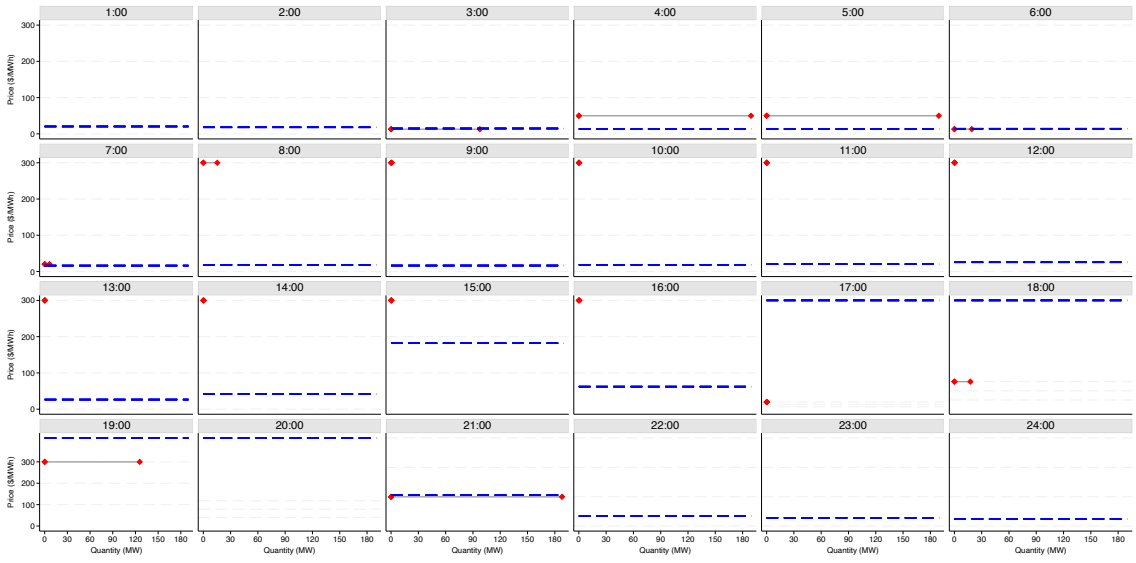

Notes: This figure plots the load bids submitted by TURQBESS_BESS1, one of the largest utility-scale battery in ERCOT. The bids are submitted on September 8, 2023 when Texas experiences significant heat, with temperatures reaching as high as 107°F in several locations. Panel (a) plots the raw bids and panel (b) plots the truncated bids at -100 dollars/MWh and 1,000 dollars/MWh. We use blue dashed line to denote the average real-time market prices for the corresponding hour in Texas on that day.

Figure A4: Map of Batteries in ERCOT

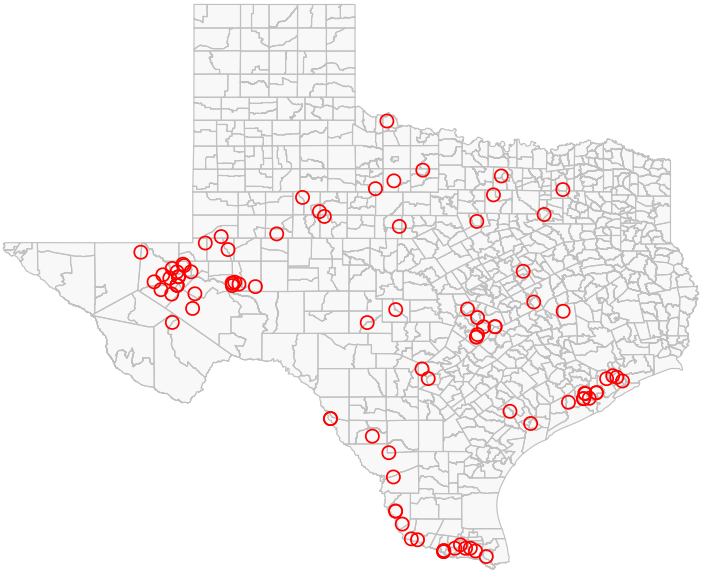

Notes: This figure plots the locations of utility-scale batteries in ERCOT in 2023. The coordinates of batteries are obtained from EIA-860.

Figure A5: Capacity Shares of Independent Batteries

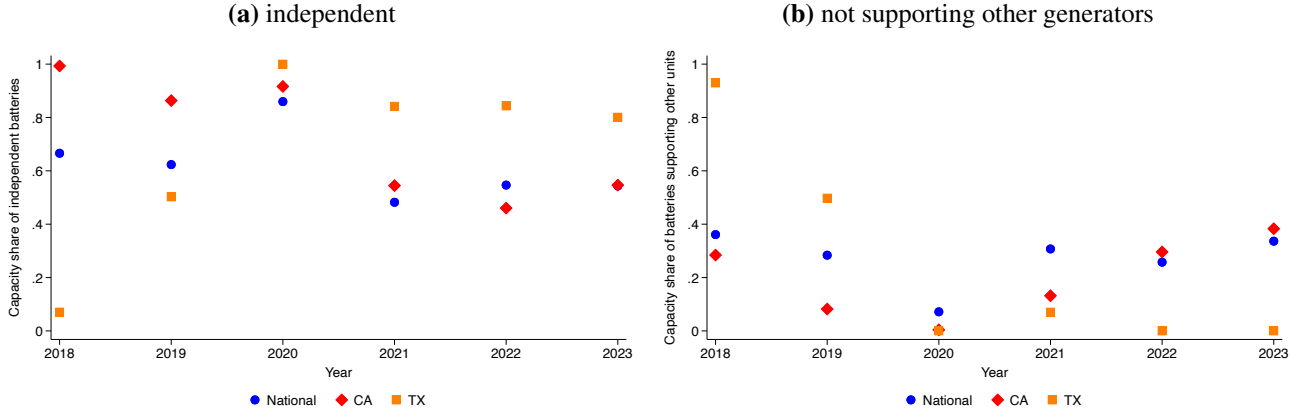

Notes: This figure plots the capacity shares of batteries that are independent (Panel (a)) and that are not supporting other generation units (Panel (b)) from 2018 to 2023. A battery is independent, defined as not being coupled with another generators. A battery directly supports another unit (mostly solar) if it is intended for dedicated generator firming or storing excess generation of other units. We plot the capacity shares nationwide (blue circles), in California (red diamonds), and in Texas (orange squares, the focus of this paper). The data source is EIA-860.

Figure A6: New Capacity of Batteries by Durations

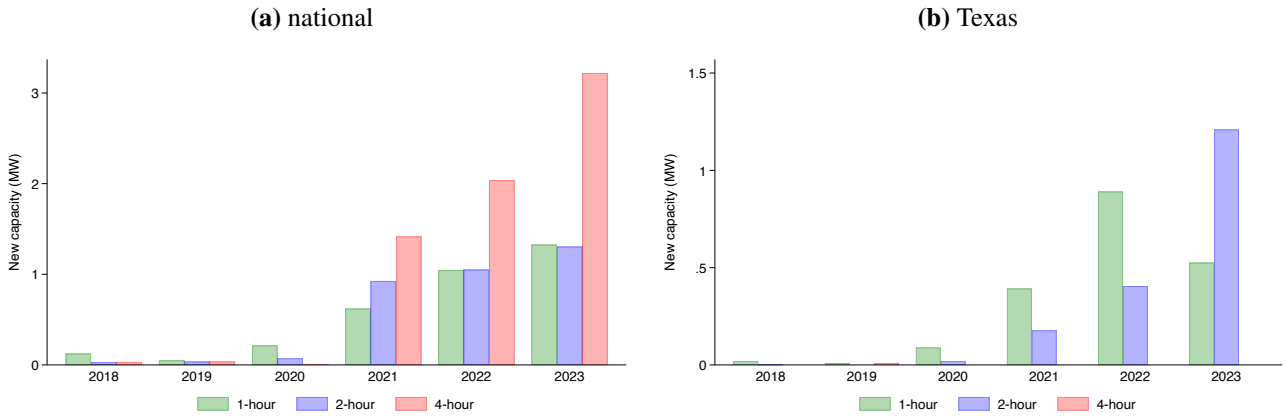

Notes: This figure plots the new capacity of batteries by durations (1-hour batteries, 2-hour batteries, 4-hour batteries) nationwide (Panel (a)) and in Texas (Panel (b)) from 2018 to 2023. A 1-hour battery could maintain its full power output for 1 hour. The data source is EIA-860.

Figure A7: Mean and Standard Deviations of Simulated Prices

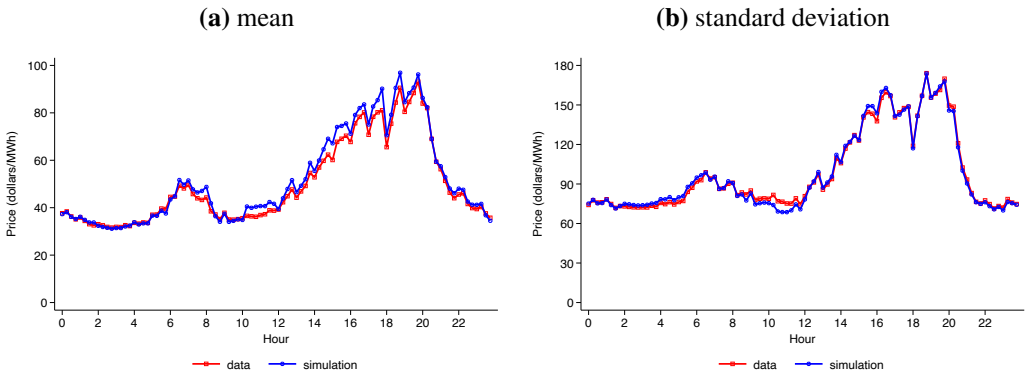

Notes: This figure compares the means (Panel (a)) and standard deviations (Panel (b)) of simulated prices and realized prices at 15-minute frequency. The statistics of simulated prices are denoted in red squares, and the statistics of realized price data are represented by blue circles.

Figure A8: Mean and Standard Deviations of Price Projections under Lead Time

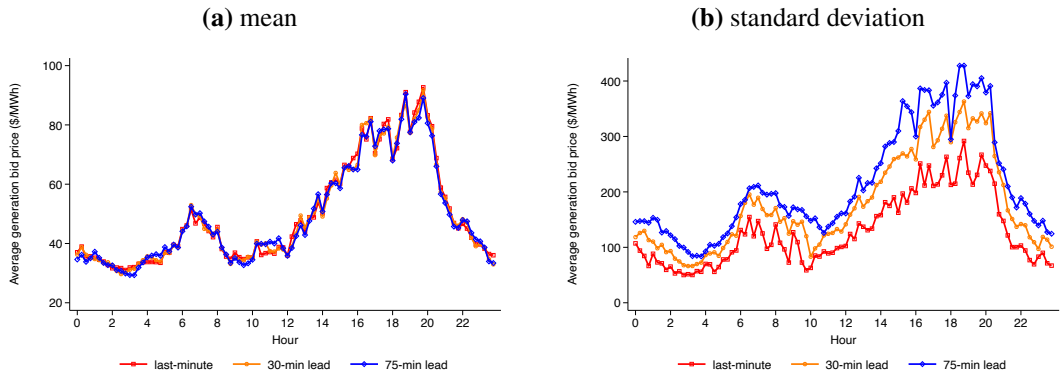

Notes: This figure plots the means (Panel (a)) and standard deviations (Panel (b)) of projected prices under various lead time, conditional on the average prices in the starting interval. Red squares represent means and standard deviations of projected prices conditional on average prices 15 minutes ago (last-minute bidding). Orange circles represent means and standard deviations of projected prices conditional on average prices 45 minutes ago (with 30-minute lead time). Blue diamonds represent means and standard deviations of projected prices conditional on average prices 90 minutes ago (with 75-minute lead time).